The Role of Blm Helicase in Homologous Recombination, Gene Conversion Tract Length, and Recombination Between Diverged Sequences in *Drosophila melanogaster*

Henry A. Ertl, Daniel P. Russo, Noori Srivastava, Joseph T. Brooks, Thu N. Dao, and Jeannine R. LaRocque[1]
Department of Human Science, Georgetown University Medical Center, Washington, DC 20057

ABSTRACT DNA double-strand breaks (DSBs) are a particularly deleterious class of DNA damage that threatens genome integrity. DSBs are repaired by three pathways: nonhomologous-end joining (NHEJ), homologous recombination (HR), and single-strand annealing (SSA). *Drosophila melanogaster Blm* (*DmBlm*) is the ortholog of *Saccharomyces cerevisiae SGS1* and human *BLM*, and has been shown to suppress crossovers in mitotic cells and repair mitotic DNA gaps via HR. To further elucidate the role of DmBlm in repair of a simple DSB, and in particular recombination mechanisms, we utilized the Direct Repeat of *white* (DR-*white*) and Direct Repeat of *white with mutations* (DR-*white.mu*) repair assays in multiple mutant allele backgrounds. *DmBlm* null and helicase-dead mutants both demonstrated a decrease in repair by noncrossover HR, and a concurrent increase in non-HR events, possibly including SSA, crossovers, deletions, and NHEJ, although detectable processing of the ends was not significantly impacted. Interestingly, gene conversion tract lengths of HR repair events were substantially shorter in *DmBlm* null but not helicase-dead mutants, compared to heterozygote controls. Using DR-*white.mu*, we found that, in contrast to Sgs1, DmBlm is not required for suppression of recombination between diverged sequences. Taken together, our data suggest that DmBlm helicase function plays a role in HR, and the steps that contribute to determining gene conversion tract length are helicase-independent.

KEYWORDS homologous recombination; homeologous recombination; gene conversion tracts; suppression of recombination between diverged sequences; *Drosophila*

DNA double-strand breaks (DSBs) must be accurately and efficiently repaired to maintain genome integrity. DSBs can be repaired through homologous recombination (HR), nonhomologous end-joining (NHEJ), or single-strand annealing (SSA) (Heyer *et al.* 2010) (Figure 1). The choice between NHEJ, HR, and SSA is determined by a variety of inputs, including cell cycle regulation (Delacote and Lopez 2008; Shrivastav *et al.* 2008; Kass and Jasin 2010) and chromatin context (Ryu *et al.* 2015; Janssen *et al.* 2016), and can also be species- and reporter-specific (Paques and Haber 1999; Do *et al.* 2014). The HR repair mechanism involves utilizing a homologous donor sequence as a template for synthesis to accurately repair the DSB. HR is initiated by 5′–3′ resection to reveal single-stranded DNA 3′ overhangs, followed by Rad51-dependent strand invasion into a homologous donor sequence (Sugawara *et al.* 1995; McIlwraith *et al.* 2000). Strand invasion results in heteroduplex DNA (hDNA) and forms a D-loop to allow for nascent strand synthesis (Figure 1, black boxes). Following DNA synthesis, there are two current models that describe alternative HR mechanisms: DSB repair (DSBR) and synthesis-dependent strand annealing (SDSA) models. In the DSBR mechanism (Figure 1A), the second end is captured after synthesis to create a double Holliday Junction (dHJ) (Szostak *et al.* 1983). Resolution of the dHJ can result in a crossover or noncrossover product. Alternatively, the SDSA mechanism involves dissociation of the newly-synthesized strand before ligation to the other DNA end (Figure 1B) (Nassif *et al.* 1994). SDSA always provides a noncrossover gene conversion product and is the preferred pathway in mitotically-dividing cells (Nassif *et al.*

doi: https://doi.org/10.1534/genetics.117.300285
Manuscript received June 15, 2017; accepted for publication September 10, 2017; published Early Online September 13, 2017.
Supplemental material is available online at www.genetics.org/lookup/suppl/doi:10.1534/genetics.117.300285/-/DC1.
[1]Corresponding author: Georgetown University, School of Nursing and Health Studies, 265 St. Mary's Hall, 3700 Reservoir Rd. NW, Washington, DC 20057. E-mail: Jan.LaRocque@georgetown.edu

1994; Rong and Golic 2003; LaRocque and Jasin 2010), while DSBR is essential for meiotically-dividing cells to generate crossover products.

Human BLM is one of five members of the evolutionarily-conserved RecQ helicase family and is important for facilitating accurate DSB repair. Mutations in human *BLM* result in Bloom syndrome (BS), which can cause cancer susceptibility, sterility, immunodeficiency, dwarfism, and premature aging (Bloom 1954; Ellis *et al.* 2008). Furthermore, BS is characterized at the cellular level by chromosomal instability leading to an elevated rate of sister chromatid exchanges and vast structural rearrangements (German *et al.* 1965; Chaganti *et al.* 1974). Mechanistically, previous studies have demonstrated BLM to have a role in DSB repair pathway choice (Grabarz *et al.* 2013), single-strand DNA resection (Gravel *et al.* 2008; Nimonkar *et al.* 2011), D-loop dissociation (Bachrati *et al.* 2006), dHJ branch migration (Karow *et al.* 2000), and dissolution (Wu and Hickson 2003; Wu *et al.* 2006). Taken together, it is evident that human BLM is involved in multiple components of both the DSBR and SDSA HR mechanisms.

Human BLM has also been shown to directly interact with mismatch repair (MMR) proteins MLH1 (Langland *et al.* 2001) and MSH6 (Pedrazzi *et al.* 2003; Yang *et al.* 2004). MMR machinery is important for maintaining genome stability by suppressing recombination of diverged sequences (*i.e.*, homeologous recombination), and repairing nucleotide mismatches in hDNA (Figure 1, black boxes) [reviewed in Spies and Fishel (2015)]. Both functions are initiated by highly conserved MSH2–MSH6 heterodimers that locate and bind to nucleotide mismatches in hDNA generated from strand invasion (Drummond *et al.* 1995). Studies in *Saccharomyces cerevisiae* have suggested that if the MMR machinery rejects the hDNA, Sgs1, the sole RecQ helicase in *S. cerevisiae*, unwinds the DNA strands (Sugawara *et al.* 2004). Additionally, similar observations between bacterial and yeast systems suggest that the Msh2–Msh3 heterodimer and Sgs1 may reject the hDNA following nascent strand annealing (Spies and Fishel 2015).

Sgs1 facilitates suppression of recombination between diverged sequences in *S. cerevisiae* (Myung *et al.* 2001), however it remains unclear whether this functionality is conserved in other organisms. Similar to Sgs1 (Sugawara *et al.* 2004), Blm was demonstrated to facilitate suppression of SSA between diverged sequences in *Drosophila* (Kappeler *et al.* 2008). However, BLM-deficient murine cells and BS cells sufficiently suppress recombination between sequences with divergence up to 1.5% (LaRocque and Jasin 2010). Interestingly, BS cells fail to suppress recombination when the sequence divergence is increased to 19% (Wang *et al.* 2016).

Drosophila has orthologs of four of the five human RecQ helicases: *DmBlm*, *WRNexo*, *DmRecQ4*, and *DmRecQ5* (Supplemental Material, Figure S1 in File S1). *DmBlm* functionality is largely conserved across species, thus is highly involved in DSB repair by HR (Kusano *et al.* 1999, 2001; Adams *et al.* 2003; McVey *et al.* 2007). In this study, we used the Direct Repeat of *white* (DR-*white*) assay to determine how DmBlm functions in DSB repair pathway usage by measuring the relative frequencies of noncrossover HR, SSA, and NHEJ repair outcomes of an I-*Sce*I-induced DSB in both null and helicase-dead *DmBlm* mutants (Figure 2A) (Do *et al.* 2014). The Direct Repeat of *white with mutations* (DR-*white.mu*) assay, which contains 28 silent nucleotide polymorphisms (SNPs) in the donor sequence increasing sequence divergence by 1.4% (Figure 2B), was used to analyze the structures of gene conversion tracts (GCTs) and determine if DmBlm plays a role in suppressing recombination between diverged sequences in multicellular systems (Do and LaRocque 2015). Our results further elucidate the role of DmBlm in multiple aspects of HR repair, and how impaired recombination mechanisms may impact the length of GCTs.

Materials and Methods

Drosophila stocks and maintenance

Drosophila were maintained on standard Nutri-fly Bloomington Formulation medium (Genesee Scientific, San Diego, CA) at 25°. DR-*white* and DR-*white.mu* transgenic stocks were previously described (Do *et al.* 2014; Do and LaRocque 2015; Delabaere *et al.* 2016) and are available upon request. I-*Sce*I transgenic stocks included either a *Drosophila Ubiquitin* promoter for constitutive expression (Preston *et al.* 2006) or *Drosophila hsp70* promoter for heat shock induction (Rong and Golic 2000; Wei and Rong 2007). *Blm* mutant stocks were as previously described: $DmBlm^{N1}$ null allele (McVey *et al.* 2007), $DmBlm^{D2}$ null allele (Boyd *et al.* 1981), and $DmBlm^{D3}$ helicase-dead allele (Boyd *et al.* 1981).

DSB repair assay

To induce DSBs, females heterozygous for Blm^{D2} containing DR-*white* or DR-*white.mu* were crossed to males heterozygous for Blm^{N1} or Blm^{D3} containing either the heat-inducible or the constitutively-active I-*Sce*I transgene. After 3 days, flies were removed. For the heat shock-inducible I-*Sce*I transgene, 0–3-day-old embryos were then heat-shocked in a 38° water bath for 1 hr. Single F1 males of either heterozygote (balanced with *TM6B*), null mutant, or helicase-dead mutant *Blm* status containing both DR-*white* (or DR-*white.mu*) and heat-inducible (or constitutively-active) I-*Sce*I transgene were crossed to five to eight *y w* females in vials. For each experiment, F2 progeny from 31 to 125 individual F1 male germlines were scored for phenotypes, as described in Figure 2 and summarized in Table S1 in File S1. For suppression of recombination between diverged sequences analysis, only the experiments in which DR-*white* and DR-*white.mu* assays were performed side-by-side were included for comparison (see Table S1 in File S1). All data from individual male germlines from these DR-*white.mu* experiments were combined by genotype to determine HR frequencies relative to DR-*white*.

Molecular analyses

For molecular analyses, one or two F2 progeny from each male germline were analyzed to avoid frequency biases attributable to potential germline jackpot events (Luria and Delbruck 1943).

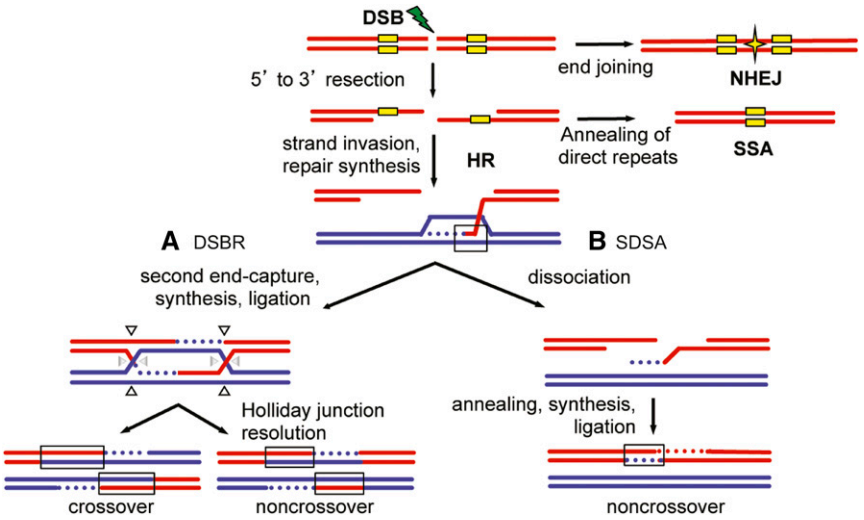

Figure 1 Models of double-strand break repair (DSBR). Double-strand breaks (DSBs) can be repaired by homologous recombination (HR), single-strand annealing (SSA), or nonhomologous end-joining (NHEJ). In NHEJ, processed ends are joined by ligation (star). HR repair is initiated by 5′–3′ resection at the DSB. If the DSB occurs between direct repeats (yellow boxes), extensive resection followed by annealing of the direct repeats results in SSA, resulting in loss of the intervening sequence. Alternatively, the resected 3′ overhang invades the homologous template (blue) to initiate repair synthesis (blue dotted line). The invaded strand may result in heteroduplex DNA (hDNA) between the red and blue sequences (black box). DNA repair synthesis is then initiated. (A) In the DSBR model, the second strand of the DSB is captured, followed by repair synthesis, and then the newly synthesized strands are ligated to form a double Holliday junction (dHJ). Depending on how the dHJ is cleaved (arrow heads), resolution can result in a crossover or a noncrossover. (B) In synthesis-dependent strand annealing (SDSA), the newly synthesized strand dissociates, anneals to the other end, the gap is filled in, and nicks ligated to result in a noncrossover product. The newly synthesized strands in both DSBR and SDSA also form hDNA. hDNA in these later HR intermediates can be repaired by mismatch repair, resulting in gene conversion (data not shown). Direct repeats are shown only for SSA for simplicity.

Genomic DNA was isolated from individual flies using 50 μl Squishing Buffer (10 mM Tris-Cl, 25 mM NaCl, and 1 mM EDTA) and Proteinase K (0.2 mg/ml). Samples were incubated at 37° for 30 m, followed by inactivation of Proteinase K by heating to 95° for 2 min (Gloor *et al.* 1993). To determine the proportion of "NHEJ with processing" events in y^+ w^- flies, *Sce.white* was PCR amplified using *Sce.white*-specific primers (forward, DR-*white*1, 5′-GTGTGAAAAATCCCGGCA-3′; reverse, DR-*white*2a 5′-TGGCAACCATCGTTGTCTG-3′) and SapphireAmp Fast PCR Master Mix (Clontech, Mountain View, CA). *Sce.white* PCR products were directly digested with I-*Sce*I restriction enzyme (New England Biolabs, Beverly, MA) and visualized on a 1% agarose gel. PCR products that failed to cleave with I-*Sce*I restriction enzyme were classified as NHEJ with processing and sent for sequencing using the DR-*white*2 primer (5′-ATG CAGGCCAGGTGCGCCTATG-3′) (Genewiz, South Plainfield, NJ) to determine the sequence of repair junctions including the presence of microhomologies. Sequences were analyzed using 4Peaks software (Nucleobytes, Aalsmeer, The Netherlands).

GCT analyses

Sce.white fragments from DR-*white.mu* HR events (y^+ w^+) were amplified with DR-*white*1 and DR-*white*1a (5′-AGACC CACGTAGTCCAGC-3′) as described above, and *Sce.white* PCR products were directly sequenced (Genewiz) with primers DR-*white* 2, DR-*white* 2a, DR-*white*1, or DR-*white*1.3 (5′-GTTTTGGGTGGGTAAGCAGG-3′) and *DR-white*1a to detect incorporations of any of the 28 silent polymorphisms from the *iwhite* donor sequence. Sequences were analyzed using 4Peaks software (Nucleobytes, Aalsmeer, The Netherlands).

Data availability

All strains and reporter constructs used in this study are available upon request. Table S1 in File S1 contains the raw data from experiments presented in Figure 3, Figure 5, and Figure S2 and Figure S5 in File S1. Table S2 in File S1 contains raw data presented in the *Results*. Figure S3 in File S1 contains the individual GCTs that are presented in Figure 4.

Results

DmBlm is involved in accurate intrachromosomal HR repair of a single break

The DR-*white* reporter determines the relative distribution of three phenotypes that represent one or more DSB repair events (Do *et al.* 2014). Briefly, DSBs are induced using an I-*Sce*I enzyme that cleaves at the I-*Sce*I recognition sequence of *Sce.white*. After I-*Sce*I expression, cleavage, and DSB repair, males are crossed to tester females to isolate and measure the relative frequencies of individual repair products in germline cells. No DSB formation, repair by intersister HR, or repair by NHEJ result in brown-bodied and white-eyed (y^+ w^-) progeny (Figure 2A, i). NHEJ with processing and microhomology-mediated end joining (MMEJ) can be detected from this group by molecular analysis at the I-*Sce*I site; loss of the I-*Sce*I recognition sequence suggests repair by NHEJ with processing (Figure 2A, i) and annealing of short homologous sequences suggests MMEJ (McVey and Lee 2008). Accurate repair by intrachromosomal noncrossover HR restores the wild-type *Sac*I site and w^+ expression, resulting in brown-bodied, red-eyed (y^+ w^+) progeny (Figure 2A, ii). NHEJ with processing leading to a perfect deletion of the 23 bp I-*Sce*I recognition sequence could result in a wild-type *Sac*I sequence and y^+ w^+ progeny. However, NHEJ with processing (this study, Table S2 in File S1), particularly deletions > 10 bp, are exceptionally rare (Do *et al.* 2014), suggesting that the vast majority of y^+ w^+ events are due to noncrossover HR. Yellow-bodied, white-eyed (y^- w^-) progeny may result from

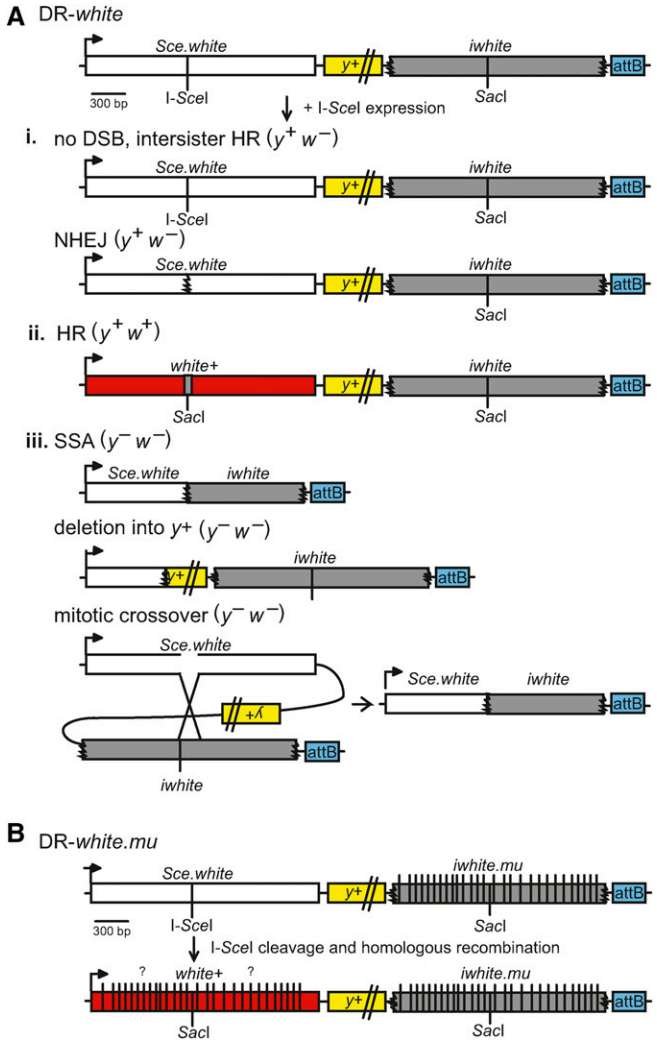

Figure 2 DR-*white* and DR-*white.mu* DSB repair assays. (A) The DR-*white* assay contains two nonfunctional direct repeats of the *white* gene. The first repeat, *Sce.white*, is nonfunctional due to the insertion of an I-*Sce*I recognition sequence into the wild-type *Sac*I recognition sequence of *white* cDNA resulting in a defective *white* gene. The second repeat, *iwhite*, is nonfunctional due to 5′ and 3′ truncations and serves as a homologous donor sequence for repair. DR-*white* is targeted using the attB sequence (blue) and integration is confirmed using *yellow* (y^+) transgene expression. DR-*white* flies are crossed with flies containing an I-*Sce*I transgene, in which expression results in DSB formation at the I-*Sce*I recognition sequence. Repair events are observed by crossing these males to *y w* tester females; progeny of this cross represent single DSB repair events of the male germline. One of three phenotypes will result depending on the repair. (i) White-eyed progeny (y^+ w^-) suggest no DSB, intersister HR, or repair by NHEJ with processing, resulting in loss of the I-*Sce*I recognition sequence. NHEJ with processing can be identified through molecular analysis. (ii) Repair by HR results in restoration of the wild-type *Sac*I site from the *iwhite* donor sequence and a red-eyed fly (y^+ w^+). (iii) Yellow-bodied, white-eyed (y^- w^-) progeny indicates repair by SSA, mitotic crossover event (indistinguishable from SSA), or an aberrant repair event that impedes y^+ expression, such as a deletion into the y^+ transgene. (B) The DR-*white.mu* assay includes the incorporation of 28 silent polymorphisms on the *iwhite.mu* donor sequence, resulting in a 1.4% increase of sequence divergence between the two direct repeats. HR gene conversion of each of the polymorphisms varies from one repair product to the next (indicated by "?"), and can be determined by molecular analyses. DR-*white*; Direct Repeat of *white*; DR-*white.mu*; Direct Repeat of *white with* loss of y^+ transgene expression by extensive end resection followed by SSA of the direct repeat sequence, a mitotic crossover event, or any aberrant repair event in which the y^+ transgene expression is lost, such as a deletion (Figure 2A, iii).

To elucidate the impact of DmBlm on DSB repair pathway distribution, we tested hetero-allelic $DmBlm^{N1/D2}$ null mutants with the DR-*white* assay and I-*Sce*I expression by heat shock. $DmBlm^{N1}$ is characterized as a 2480 bp deletion that includes the start codon (McVey *et al.* 2007), and $DmBlm^{D2}$ is a nonsense mutation (Kusano *et al.* 2001). Both the $DmBlm^{N1}$ and $DmBlm^{D2}$ alleles are characterized as genetic nulls (McVey *et al.* 2007). In accordance with trends reported with the Rr3 DSB repair assay in a previous study (Johnson-Schlitz *et al.* 2007), we measured a ~50% decrease of noncrossover HR repair events from 22.6% in $DmBlm^{N1}$ heterozygote controls to 11.7% in $DmBlm^{N1/D2}$ null mutants ($P < 10^{-12}$, Student's *t*-test) (Figure 3A). Furthermore, there was a threefold increase of y^- w^- flies from 3.1% in the $DmBlm^{N1}$ heterozygotes to 10.1% in the $DmBlm^{N1/D2}$ null mutants ($P < 10^{-13}$, Student's *t*-test) (Figure 3A). Notably, because the study by Johnson-Schlitz *et al.* (2007) utilized a constitutively-active I-*Sce*I transgene with their Rr3 DSB repair assay, we also tested the constitutively-active I-*Sce*I transgene in DR-*white* and observed a similar decrease in noncrossover HR and a compensatory increase in y^- w^- (Figure S2 in File S1). Finally, we detected a relatively small, yet significant, increase in the frequency of the y^+ w^- class from 74.3% in $DmBlm^{N1}$ heterozygotes to 78.3% in $DmBlm^{N1/D2}$ null mutants ($P < 0.05$, Student's *t*-test) (Figure 3A). Within this y^+ w^- pool, 8.1% of the repair events from $DmBlm^{N1}$ heterozygotes were due to NHEJ with processing, which was not significantly different from the 5.9% NHEJ with processing repair events in $DmBlm^{N1/D2}$ null mutants ($P = 0.6$, Fisher's exact test) (Table S2 in File S1). Also within the NHEJ with processing events, there were no significant differences in the proportion of events with microhomologies between $DmBlm^{N1}$ heterozygotes (23/38 NHEJ events contained microhomologies) and $DmBlm^{N1/D2}$ null mutants (22/34 NHEJ events contained microhomologies) ($P = 0.8$, Fisher's exact test) (Table S2 in File S1).

DSB repair pathway distribution is DmBlm helicase-dependent

To specifically test the DmBlm helicase enzymatic function in our system, we used the DR-*white* assay with $DmBlm^{D2/D3}$ helicase-dead mutants. The $DmBlm^{D3}$ allele is characterized as a missense mutation (Kusano *et al.* 2001) that alters a critical motif for nucleotide cofactor binding and hydrolysis, thus encoding DmBlm protein with impaired helicase function (McVey *et al.* 2007). Similar to the experiments using null mutants, the noncrossover HR frequency decreased by ~50% from 26.5% in $DmBlm^{D3}$ heterozygote controls to

mutations; DSB, double-strand break; HR, homologous recombination; NHEJ, nonhomologous end-joining; SSA, single-strand annealing.

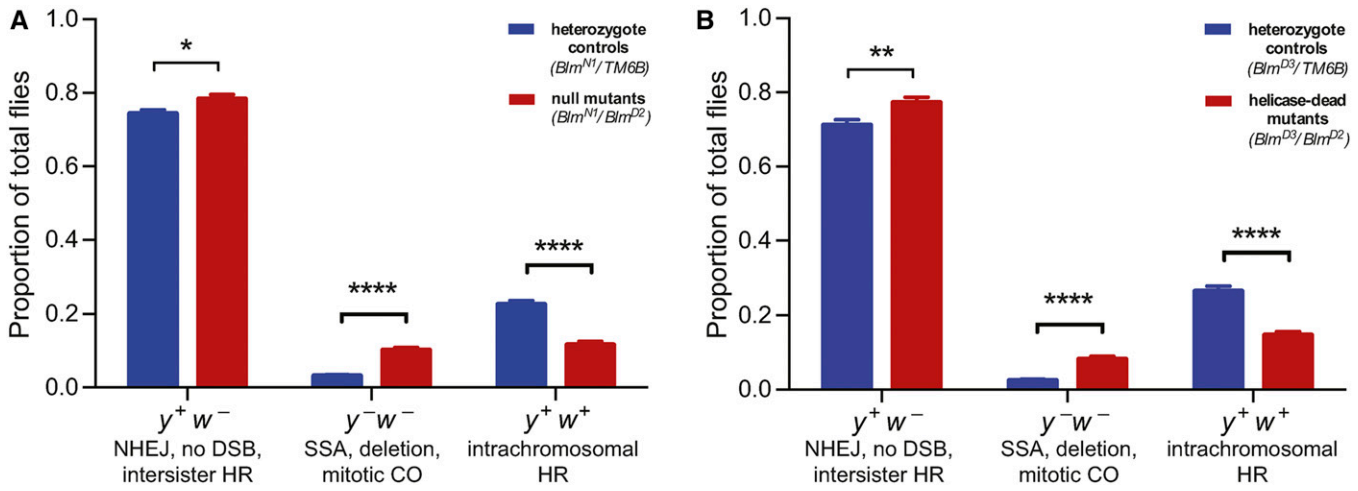

Figure 3 DmBlm impacts DSB repair pathway usage. (A) I-*Sce*I heat shock-induced DSB repair events in a $DmBlm^{N1/D2}$ null mutant background (red; $n = 94$) compared to $DmBlm^{N1}$ heterozygote controls (blue; $n = 125$). Results shown are averages and SEM of individual male germline events compiled from five independent experiments. * $P < 0.05$ and **** $P < 0.0001$ by unpaired Student's *t*-test. (B) I-*Sce*I heat shock-induced DSB repair events in a $DmBlm^{D3/D2}$ helicase-dead mutant background (red; $n = 52$) compared to $DmBlm^{D3}$ heterozygote controls (blue; $n = 59$). Results shown are averages and SEM of individual male germline events compiled from three independent experiments. ** $P < 0.01$ and **** $P < 0.0001$ by unpaired Student's *t*-test. CO, crossover; DSB, double-strand break; HR, homologous recombination; NHEJ, nonhomologous end-joining; SSA, single-strand annealing.

14.6% in $DmBlm^{D2/D3}$ helicase-dead mutants ($P < 10^{-9}$, Student's *t*-test). Furthermore, the frequency of the $y^- w^-$ class increased threefold from 2.4% in $DmBlm^{D3}$ heterozygotes to 8.2% in $DmBlm^{D2/D3}$ helicase-dead mutants ($P < 10^{-7}$, Student's *t*-test), and the frequency of $y^+ w^-$ flies slightly increased from 71.1% in $DmBlm^{D3}$ heterozygotes to 77.2% in $DmBlm^{D2/D3}$ helicase-dead mutants ($P < 0.01$, Student's *t*-test) (Figure 3B). Within the $y^+ w^-$ pool, 11.3% of the repair events from $DmBlm^{D3}$ heterozygotes were due to NHEJ with processing, which was not significantly different from the 8.1% NHEJ with processing repair events in $DmBlm^{D2/D3}$ helicase-dead mutants ($P = 0.6$, Fisher's exact test) (Table S2 in File S1). These results indicate the role of DmBlm in multiple DSB repair pathway distributions to be, at least partially, helicase-dependent.

GCTs are significantly shorter in DmBlm null but not helicase-dead mutants

Gene conversion results from a noncrossover HR repair event and can have significant impacts on genome stability and evolution [reviewed in Chen *et al.* (2007)]. To further investigate the noncrossover HR deficiencies observed in *DmBlm* mutants, we quantified HR GCT lengths of *DmBlm* null and helicase-dead mutants by molecular analysis using the DR-*white.mu* assay (Do *et al.* 2014). By sequencing the recipient fragment, *Sce.white*, we were able to determine the structure and length of GCTs based on the presence or absence of SNPs from the donor sequence, *iwhite.mu* (Figure 2B).

We determined $DmBlm^{N1}$ heterozygotes to have a mean GCT length of 374.8 ± 40.3 bp, and this dropped substantially to 146.9 ± 35.9 bp in $DmBlm^{N1/D2}$ null mutants ($P < 10^{-4}$, Student's *t*-test) (Figure 4A and Figure S3 in File S1). Moreover, of all $DmBlm^{N1}$ heterozygote GCTs analyzed ($n = 59$), five (8.5%) of the GCTs were limited to the *Sac*I site, 36 (61.0%) were unidirectional, and 18 (30.5%) were bidirectional (Figure 4C and Figure S3 in File S1). In contrast, of all $DmBlm^{N1/D2}$ null mutant GCTs analyzed ($n = 51$), 22 (43.1%) of the GCTs were limited to the *Sac*I site, 19 (37.3%) were unidirectional, and 10 (19.6%) were bidirectional (Figure 4C and Figure S3 in File S1). Interestingly, while the proportion of bidirectional GCTs does not differ between $DmBlm^{N1}$ heterozygotes and $DmBlm^{N1/D2}$ null mutants ($P = 0.5$, Fisher's exact test), the two genotypes significantly differ in the proportion of GCTs limited to the *Sac*I site ($P < 0.001$, Fisher's exact test) and unidirectional GCTs ($P < 0.001$, Fisher's exact test). Two (3.4%) discontinuous tracts were observed in $DmBlm^{N1}$ heterozygote controls and four (7.8%) were observed in $DmBlm^{N1/D2}$ null mutant flies ($P = 0.4$, Fisher's exact test) (Figure S3 in File S1). Finally, neither $DmBlm^{N1}$ heterozygote ($P = 0.1$, Student's *t*-test) nor $DmBlm^{N1/D2}$ null mutant GCTs ($P = 0.7$, Student's *t*-test) exhibited significant biases in either direction of the *Sac*I site (Figure S4 in File S1).

To test whether the apparent effects of DmBlm on GCT length are helicase-dependent, we also analyzed GCTs from *DmBlm* helicase-dead mutants. Interestingly, the mean GCT length for $DmBlm^{D2}$ heterozygote controls was longer than the $DmBlm^{D3/D2}$ helicase-dead mutants (338.7 ± 47.0 bp *vs.* 235.8 ± 38.3 bp), but the difference did not reach significance ($P = 0.09$) (Figure 4B and Figure S3 in File S1). Similarly, the mean GCT length in $DmBlm^{D3}$ heterozygote controls was 283.4 ± 32.1 bp, which did not significantly differ from that of $DmBlm^{D3/D2}$ helicase-dead mutants, 235.8 ± 38.3 bp ($P = 0.3$, Student's *t*-test) (Figure 4B and Figure S3 in File S1). These results suggest that the decrease in GCT lengths in *DmBlm* mutants is mostly helicase-independent.

Of all $DmBlm^{D2}$ heterozygote GCTs analyzed ($n = 59$), 10 (16.9%) of the GCTs were limited to the *Sac*I site, 35 (59.3%) were unidirectional, and 14 (23.7%) were bidirectional (Figure 4C and Figure S3 in File S1). Of all $DmBlm^{D3}$

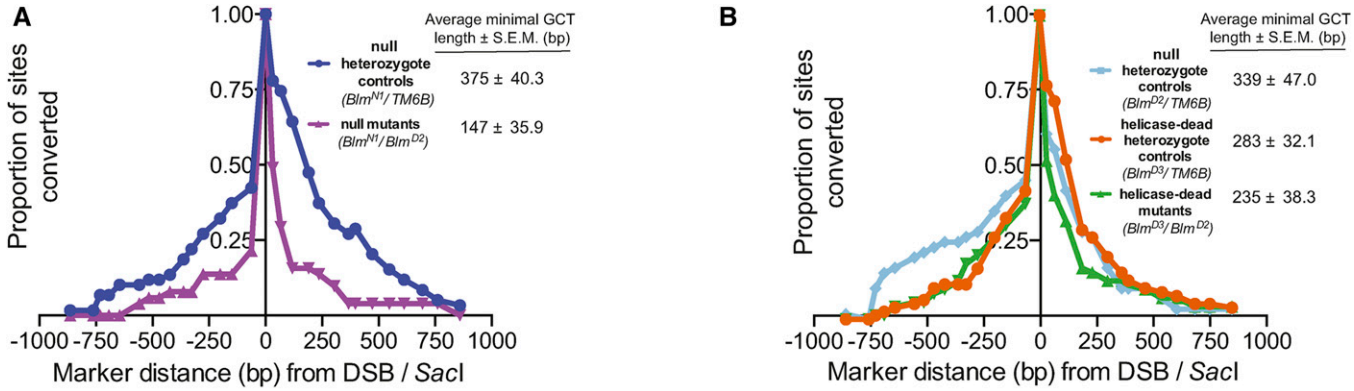

C

Number of GCTs (% of total)

DmBlm^{N1} heterozygotes	null mutants	DSB / *Sac*I	*DmBlm*^{D2} heterozygotes	*DmBlm*^{D3} heterozygotes	helicase-dead mutants
5 (8)	22 (43)		10 (17)	10 (13)	21 (30)
28 (47)	16 (31)		22 (37)	32 (41)	22 (31)
8 (14)	3 (6)		13 (22)	8 (10)	13 (18)
18 (31)	10 (20)		14 (24)	28 (36)	15 (21)
Total: 59 (100)	51 (100)		59 (100)	78 (100)	71 (100)

Figure 4 DmBlm impacts gene conversion tract length independently of helicase function. Intrachromosomal noncrossover HR events using the DR-*white.mu* assay were isolated and the GCT direction and length were determined. (A) The proportions of SNP sites converted are displayed for *DmBlm*^{N1} heterozygote control HR events (blue; $n = 59$) and *DmBlm*$^{N1/D2}$ null mutant HR events (purple; $n = 51$). The average distance converted and SEM (base pair) to the left and to the right of the *Sac*I site/DSB (0) is given for both genotypes. Data are from two independent experiments. (B) The proportions of SNP sites converted are displayed for *DmBlm*^{D2} heterozygote control HR events (light blue; $n = 59$), *DmBlm*^{D3} heterozygote control HR events (orange; $n = 78$) and *DmBlm*$^{D3/D2}$ helicase-dead mutant HR events (green; $n = 71$). The average distance and SEM converted (base pair) to the left and to the right of the *Sac*I site/DSB (0) is given for both genotypes. Data are from four independent experiments. (C) Classes of gene conversion tracts from combined DR-*white.mu* assay experiments in *DmBlm*$^{N1/D2}$ null mutants (left) and *DmBlm*$^{D3/D2}$ helicase-dead mutants (right) and the respective heterozygote control. Each tract was grouped into one of four classes (represented graphically in descending order): conversion of only the DSB/*Sac*I site, conversion to the right of the DSB/*Sac*I site (> 32 bp; unidirectional), conversion to right of the DSB/*Sac*I site (> 63 bp; unidirectional), and conversion to both sides of the break (bidirectional). DR-*white.mu*; Direct Repeat of *white with mutations*; DSB, double-strand break; GCT, gene conversion tract; HR, homologous recombination; SNP, single nucleotide polymorphism.

heterozygote GCTs analyzed ($n = 78$), 10 (12.8%) of the GCTs were limited to the *Sac*I site, 40 (51.3%) were unidirectional, and 28 (35.9%) were bidirectional (Figure 4C and Figure S3 in File S1). Of all *DmBlm*$^{D3/D2}$ helicase-dead mutant GCTs analyzed ($n = 71$), 21 (29.6%) of the GCTs were limited to the *Sac*I site, 35 (49.3%) were unidirectional, and 15 (21.1%) were bidirectional (Figure 4C and Figure S3 in File S1). Between *DmBlm*^{D2} heterozygotes and *DmBlm*$^{D3/D2}$ helicase-dead mutants, the proportions of bidirectional ($P = 0.8$, Fisher's exact test) and unidirectional ($P = 0.3$, Fisher's exact test) GCTs did not differ. Similarly, between *DmBlm*^{D3} heterozygotes and *DmBlm*$^{D3/D2}$ helicase-dead mutants, the proportions of bidirectional ($P = 0.2$, Fisher's exact test) and unidirectional ($P = 0.6$, Fisher's exact test) GCTs did not differ. However, the *DmBlm*^{D3} heterozygotes and *DmBlm*$^{D3/D2}$ helicase-dead mutants did significantly differ in the proportion of GCTs limited to the *Sac*I site ($P < 0.05$, Fisher's exact test), although there was no statistical different between *DmBlm*^{D2} heterozygotes and *DmBlm*$^{D3/D2}$ helicase-dead mutants ($P = 0.1$, Fisher's exact test). One (1.7%) and four (5.1%) discontinuous tracts were observed in *DmBlm*^{D2} and *DmBlm*^{D3} heterozygote controls, respectively. Two (2.8%) discontinuous tracts were observed in *DmBlm*$^{D3/D2}$ helicase-dead mutants ($P = 1.0$ and 0.7, Fisher's exact test comparing D2 heterozygotes to helicase-dead mutants and D3 heterozygotes to helicase-dead mutants, respectively) (Figure S3 in File S1). Finally, similar to the *DmBlm* null mutant experiment, neither *DmBlm*^{D2} heterozygote ($P = 0.1$, Student's *t*-test), *DmBlm*^{D3} heterozygote ($P = 0.1$, Student's *t*-test), nor *DmBlm*$^{D3/D2}$ helicase-dead mutant GCTs ($P = 0.9$, Student's *t*-test) exhibited significant biases in either direction of the *Sac*I site (Figure S4 in File S1).

DmBlm mutants suppress noncrossover recombination between diverged sequences

A previous study found that *DmBlm*$^{D2/D3}$ helicase-dead mutants failed to suppress SSA between diverged sequences, suggesting a function for the DmBlm helicase in SSA hDNA

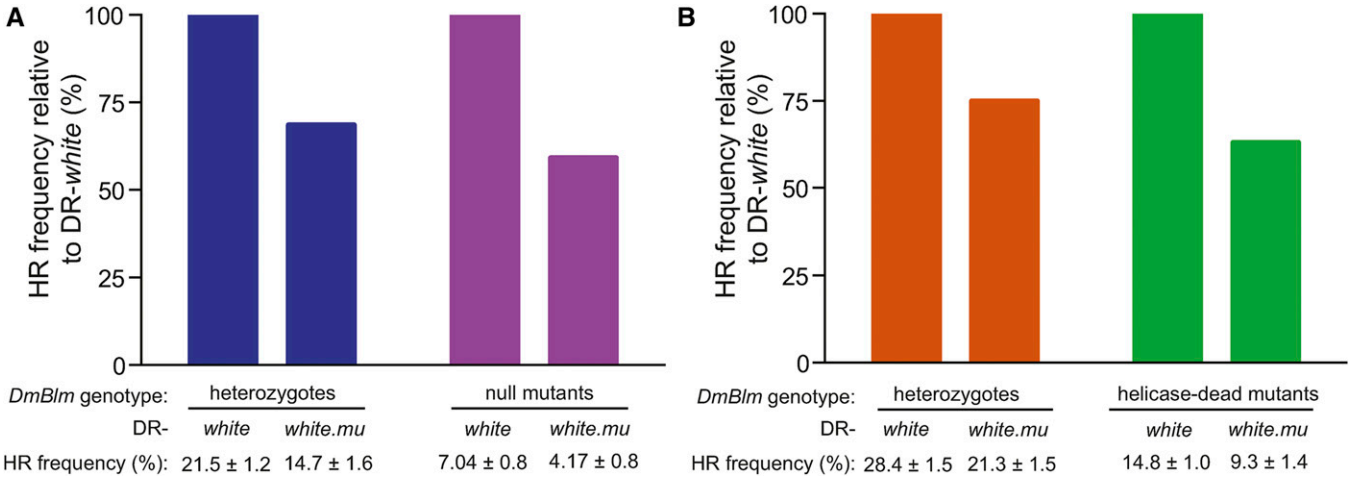

Figure 5 Relative recombination frequencies between homologous and diverged sequences are unaltered in *DmBlm* mutants. Relative recombination frequencies between homologous and diverged sequences were determined using DR-*white* and DR-*white.mu*, respectively, in (A) $DmBlm^{N1}$ heterozygote controls and $DmBlm^{N1/D2}$ null mutants, and (B) $DmBlm^{D3}$ heterozygote controls and $DmBlm^{D3/D2}$ helicase-dead mutants. Average HR frequencies (with SEM) were compiled from individual germlines from two independent experiments and are presented below the graphs (and in Table S1 in File S1). Average HR frequencies relative to DR-*white* are plotted. DR-*white*; Direct Repeat of *white*; DR-*white.mu*; Direct Repeat of *white with mutations*; HR, homologous recombination.

rejection (Kappeler *et al.* 2008). With the DR-*white* and DR-*white.mu* assays, we tested suppression of noncrossover HR between diverged sequences by directly measuring the proportion of HR between homologous (DR-*white*) and diverged (DR-*white.mu*) sequences. Our earlier study demonstrated that wild-type $DmBlm^{+/+}$ flies suppressed HR frequency measured with DR-*white.mu* by 31.5% relative the HR frequency measured with DR-*white* (Do *et al.* 2014). Furthermore, *msh6* mutants failed to suppress recombination with the DR-*white.mu* assay relative to that with DR-*white*, suggesting this effect to be MMR machinery-dependent (Do and LaRocque 2015).

To determine if DmBlm suppresses recombination of diverged sequences similar to *S. cerevisiae* Sgs1 (Myung *et al.* 2001) and *Drosophila* Msh6, we tested these effects in $DmBlm^{N1/D2}$ null mutants. Nearly identical to $DmBlm^{+/+}$ flies, the noncrossover recombination frequency of $DmBlm^{N1}$ heterozygote controls with diverged sequences was suppressed by 31.5% relative to HR with homologous sequences (21.5 ± 1.2% HR with DR-*white* and 14.7 ± 1.6% HR with DR-*white.mu*; $P < 0.001$, Student's *t*-test) (Figure 5A). Similarly, $DmBlm^{N1/D2}$ null mutants suppressed noncrossover HR with diverged sequences by 40.8% compared to HR with homologous sequences (7.0 ± 0.8% HR with DR-*white* and 4.2 ± 0.8% HR with DR-*white.mu*; $P < 0.05$, Student's *t*-test) (Figure 5A). The relative frequencies of the other phenotypic classes were also consistent regardless of *DmBlm* status or the presence of a homologous or diverged donor sequence (Figure S5 in File S1).

Since the previously mentioned study by Kappeler *et al.* (2008) tested $DmBlm^{D3/D2}$ helicase-dead mutants, we repeated this assay in a $DmBlm^{D3/D2}$ helicase-dead genetic background. The recombination frequency in $DmBlm^{D3}$ heterozygote controls with diverged sequences was suppressed by 25.1% relative to HR with homologous sequences (28.4 ± 1.5% HR with DR-*white* and 21.3 ± 1.5% HR with DR-*white.mu*; $P < 0.01$, Student's *t*-test) (Figure 5B). Similar to $DmBlm^{N1/D2}$ null mutants, $DmBlm^{D3/D2}$ helicase-dead mutants also suppressed noncrossover recombination frequency by 36.9% relative to HR with homologous sequences (14.8 ± 1.0% HR with DR-*white* and 9.3 ± 1.4% HR with DR-*white.mu*; $P < 0.01$, Student's *t*-test) (Figure 5B).

Discussion

DmBlm impacts DSB repair pathway distribution by its involvement in HR

DmBlm promotes efficient and accurate repair of DNA gaps by the SDSA HR pathway (Adams *et al.* 2003). Johnson-Schlitz *et al.* (2007) previously found that *DmBlm* mutants suppress interhomolog HR and compensate by increasing SSA repair pathway usage in their Rr3 DSB repair assay. In this current study, we utilize the DR-*white* assay to demonstrate consistent results with a DSB detector assay that measures intrachromosomal noncrossover HR repair. Furthermore, *DmBlm* null and helicase-dead mutants both exhibited a threefold increase of $y^-\ w^-$ flies, which may be explained by a shift from noncrossover HR to crossover HR, as observed by the increase in crossovers and flanking deletions associated with *DmBlm* deficiencies (Johnson-Schlitz and Engels 2006; McVey *et al.* 2007), although these events cannot be precisely identified molecularly in our assay (see Figure 2A, iii).

The statistically significant increase in $y^+\ w^-$ repair events in DmBlm mutants could be due to a shift from noncrossover HR to NHEJ events. However, neither the relative proportion of NHEJ with processing events nor NHEJ with microhomology events differ between *DmBlm* null and helicase-dead mutants and the respective heterozygote controls (Table S2 in File S1). Given the sparse evidence connecting DmBlm functionally to the NHEJ pathway, this increase is more likely

due to cell death of failed intrachromosomal HR repair events in the germline, thus causing a proportional increase in this class (y^+ w^-). It is also possible that the increase in y^+ w^- flies reflects a shift from intrachromosomal noncrossover HR to intersister HR using the *Sce.white* sequence as a donor sequence. However, these events cannot be molecularly distinguished from "no DSB" events, which retain the I-*Sce*I recognition sequence. Overall, these data demonstrate the ability of DR-*white* to simultaneously capture multiple types of repair events and identify compensatory pathway shifts in mutant backgrounds, as observed previously in mutants required for HR (*e.g.*, *DmRad51*) (Do *et al.* 2014).

In general, $DmBlm^{N1/D2}$ null and $DmBlm^{D3/D2}$ helicase-dead genetic backgrounds had similar effects on DSB repair pathway usage detected with the DR-*white* assay (Figure 3). These results are consistent with a previous study in which $DmBlm^{D3/D2}$ helicase-dead flies exhibited increased ionizing radiation sensitivity, although interestingly not to the extent of $DmBlm^{N1/N1}$ null mutants (McVey *et al.* 2007). Furthermore, BLM helicase-deficient human cells were recently shown to suppress the elongation of branch migration and dHJ crossovers (Suzuki *et al.* 2016). Taken together, these results indicate that the helicase enzymatic activity is necessary for many functions of DmBlm in DSB repair.

A helicase-independent role of DmBlm in homologous recombination impacts GCT lengths

$DmBlm^{N1/D2}$ null mutants exhibit a striking decrease in GCT lengths compared to $DmBlm^{N1}$ heterozygote controls (Figure 4A). However, $DmBlm^{D3/D2}$ helicase-dead mutant GCT lengths do not differ significantly from $DmBlm^{D2}$ heterozygote controls or $DmBlm^{D3}$ heterozygote controls, suggesting this effect to be mostly helicase-independent (Figure 4B). Others have reported the $DmBlm^{D3}$ allele to be antimorphic in SDSA gap repair assays (McVey *et al.* 2007). In this study, the average GCT lengths in $DmBlm^{D3}$ heterozygote controls were lower than in both $DmBlm^{N1}$ and $DmBlm^{D2}$ heterozygote controls, although this difference does not reach statistical significance ($P = 0.08$ and $P = 0.33$, respectively; Student's *t*-test). Additionally, we see no statistically significant difference in noncrossover HR frequency in $DmBlm^{N1/D2}$ and $DmBlm^{D3/D2}$ mutants ($P = 0.06$). However, although our data does not reach statistical significance, the trends we report here suggest that the $DmBlm^{D3}$ allele may be a semidominant phenotype, which may be more prevalent when assaying for gap repair (McVey *et al.* 2007).

Considering the impact of DmBlm on GCT length, there are multiple mechanisms that could contribute to GCT tract length, of which DmBlm may play a role. Based on the current SDSA and DSBR pathway models, GCT lengths may be affected by: (1) end resection, (2) branch migration, (3) strand synthesis, and/or (4) DNA mismatch repair. First, following a DSB, 5′–3′ resection determines how much sequence information is available for invasion into the homologous donor sequence. If the resection to GCT length relationship was isolated, less resection could result in shorter GCT lengths, and vice versa. Indeed, *S. cerevisiae exo1* mutants, which have reduced end resection, are associated with crossovers and shorter GCTs (Yin and Petes 2014). However, contrary to this model, *S. cerevisiae yku70* mutants with increased resection and *mre11* mutants with reduced resection have GCTs similar to wild-type in a chromosomal context (Krishna *et al.* 2007). A previous study outlined two DNA end resection machinery complexes in human cells that both involve BLM (Nimonkar *et al.* 2011). One pathway requires BLM helicase functionality to unwind DNA to allow for resection by DNA2, but the other pathway involves EXO1 end resection that is stimulated by BLM independently of the helicase functionality (Nimonkar *et al.* 2008, 2011). Our results corroborate a helicase-independent role for DmBlm in end resection, which could ultimately impact GCT length.

Second, branch migration of recombination intermediates may also affect GCT length. DmBlm is known to promote SDSA by facilitating D-loop branch migration in order for the invading strand to dissociate (McVey *et al.* 2004; Weinert and Rio 2007). Given this function, a common phenotype associated with *DmBlm* mutants is increased mitotic crossovers (Johnson-Schlitz and Engels 2006; McVey *et al.* 2007), which could result from an inability to resolve recombination intermediates. In *S. cerevisiae*, mitotic crossovers are more often associated with longer GCTs (Jinks-Robertson *et al.* 1993; Symington *et al.* 2000). Therefore, it is plausible that a subset of noncrossover HR events associated with longer GCTs due to extensive branch migration are resolved as y^- w^- crossover products, which would explain our results of a decrease in noncrossover HR and a loss of longer GCTs in *DmBlm* null mutants.

Third, repair synthesis may impact GCT length. In *S. cerevisiae*, DSB repair requires both leading and lagging DNA polymerase functionality (Holmes and Haber 1999). *S. cerevisiae* lacking DNA polymerase δ have shorter GCT lengths, suggesting this effect to be correlated with primed DNA synthesis lengths (Maloisel *et al.* 2008). DmBlm lacks polymerase enzymatic properties, thus is unlikely to directly impact repair synthesis. However, the proposed DmBlm DNA end resection function may indirectly affect subsequent nascent strand DNA synthesis and therefore GCT length.

Lastly, GCT lengths may also be affected if MMR machinery is unable to correct base pair mismatches in hDNA [reviewed in Spies and Fishel (2015)]. Failure to convert mismatches in hDNA to the recipient sequence strand would result in longer GCTs. However, our result that *DmBlm* null mutants have shorter GCTs suggests that DmBlm is not involved in conversion of hDNA to the recipient strand sequence. This result may be consistent with previous studies that have shown *S. cerevisiae sgs1* mutants (Lo *et al.* 2006) and BS human cells (Langland *et al.* 2001) to have fully functional base pair mismatch repair capabilities. Given the complexity of mechanisms that drive GCT length and the versatility of the DmBlm protein, more work is needed to isolate and quantify the determinants of GCT length and structure in multicellular organisms.

The GCTs analyzed in *DmBlm* mutants are a subset of DSB repair events that are able to complete HR (~50% of the events in heterozygote controls). It is possible that the detectable mean GCT lengths with the DR-*white.mu* assay are skewed in *DmBlm* mutants since we are only measuring viable y^+w^+ progeny. For example, mechanisms that lead to longer GCT HR repair events in the absence of DmBlm may cause cell death, or be more susceptible to becoming the aberrant repair products frequently observed in *DmBlm* null mutants (Johnson-Schlitz and Engels 2006). These mechanisms would result in the y^- w^- phenotype as opposed to the y^+ w^+ HR phenotype. However, if we were unable to detect the longer GCT lengths due to the HR impairment in *DmBlm* mutants, we would expect $DmBlm^{D3}$ helicase-dead mutants to similarly exhibit shorter mean GCT lengths compared to $DmBlm^{D3}$ or $DmBlm^{D2}$ heterozygote controls. Additionally, extensive gene conversion beyond the *iwhite* donor sequence may also skew the relative phenotype distribution by resulting in a y^+ w^- phenotype that contains a converted *Sac*I sequence at the repair junction, instead of a y^+ w^+ HR event. Importantly, we did not observe a *Sac*I conversion event in any repair events from y^+ w^- flies, suggesting that extensive gene conversion is unlikely.

DmBlm is not involved in suppression of noncrossover recombination between diverged sequences

Our DR-*white* and DR-*white.mu* assays can directly measure the ratio of noncrossover HR between homologous and 1.4% diverged sequences, respectively (Do *et al.* 2014). In both $DmBlm^{N1/D2}$ null and $DmBlm^{D2/D3}$ helicase-dead mutants, the ratio of noncrossover HR between homologous and diverged sequences was not significantly affected, suggesting that DmBlm is not involved in the suppression of recombination between diverged sequences. At similar levels of sequence divergence, BLM is dispensable for suppressing recombination between diverged sequences in both human and murine cells as well (LaRocque and Jasin 2010), but the sole RecQ helicase in *S. cerevisiae*, Sgs1, is necessary to suppress recombination of sequences with $\leq$ 9% divergence (Myung *et al.* 2001).

Whereas *S. cerevisiae* and *Escherichia coli* bacteria have only one known RecQ helicase, fruit flies, humans, and mice all have at least four RecQ helicase paralogs (Figure S1 in File S1), suggesting duplicate gene evolution in metazoans. Two possible outcomes of duplicate gene evolution are: (1) subfunctionalization, the duplicated genes each retain different subfunctions of the ancestral gene, and (2) neofunctionalization, one of the duplicated genes acquires a novel functionality while the other copy retains the ancestral functionality (Lynch and Conery 2000). Either of these gene evolutionary histories can explain why the BLM ortholog in species with one RecQ helicase suppresses recombination of sequences with nucleotide divergence $<$ 9%, but not in species with multiple RecQ helicases. Additionally, high conservation of the helicase domain of RecQ helicases within and across species may allow for partial functional redundancy in species with multiple RecQ helicases (Kitao *et al.* 1998). To elucidate the collective roles of the RecQ helicase protein family in suppressing recombination of diverged sequences, future experiments are needed in other RecQ helicases within *Drosophila*, as well as in other genetically-tractable model organisms with multiple RecQ helicases, such as *Caenorhabditis elegans* (Jung *et al.* 2014; Ryu and Koo 2016), *Danio rerio* (Xie *et al.* 2007), and *Arabadopsis thaliana* (Knoll and Puchta 2011).

In contrast to our data quantifying recombination between diverged sequences, Kappeler *et al.* (2008) demonstrated that $DmBlm^{D2/D3}$ helicase-dead mutants failed to suppress SSA with sequence divergences $<$ 0.5%. Sequence divergence used in these two assays are similar, thus this discrepancy may most likely be attributed to the differences in the SSA and HR mechanisms. HR and SSA are both initiated by 5′ to 3′ resection and utilize similar components of the MMR machinery to ensure sufficient homology before undergoing recombination. Furthermore, the SDSA HR model and SSA share the *S. cerevisiae* Rad1-Rad10 nuclease-dependent 3′ flap processing step to stabilize hDNA (Fishman-Lobell and Haber 1992; Ivanov and Haber 1995; Mazon *et al.* 2012). However, multiple intermediate steps in the HR pathway that differ from the SSA pathway may consequently affect hDNA rejection mechanisms. For example, Rad51 coats the 3′ single-strand DNA and facilitates invasion into a homologous donor sequence (McIlwraith *et al.* 2000), and is then disassembled by a complex including *S. cerevisiae* Rad54 (Wright and Heyer 2014), the *C. elegans* Rad51 ortholog RFS-1, and DNA helicase HELQ-1 (Ward *et al.* 2010). These upstream steps of hDNA rejection are not necessary for SSA, and it is unclear how these differences between HR and SSA pathways may alter the respective recombination suppression mechanisms.

Acknowledgments

We thank the Sekelsky and McVey laboratories for reagents and members of the LaRocque laboratory for discussion. This research was supported by National Institutes of Health grant 1R15-GM-110454-01 (to J.R.L.) and in part by the Georgetown Undergraduate Research Opportunities Program (J.T.B. and N.S.).

Literature Cited

Adams, M. D., M. McVey, and J. Sekelsky, 2003 *Drosophila* BLM in double-strand break repair by synthesis-dependent strand annealing. Science 299: 265–267.

Bachrati, C. Z., R. H. Borts, and I. D. Hickson, 2006 Mobile D-loops are a preferred substrate for the bloom's syndrome helicase. Nucleic Acids Res. 34: 2269–2279.

Bloom, D., 1954 Congenital telangiectatic erythema resembling lupus erythematosus in dwarfs; probably a syndrome entity. AMA Am. J. Dis. Child. 88: 754–758.

Boyd, J. B., M. D. Golino, K. E. S. Shaw, C. J. Osgood, and M. M. Green, 1981 Third-chromosome mutagen-sensitive mutants of *Drosophila melanogaster*. Genetics 97: 607–623.

Chaganti, R. S., S. Schonberg, and J. German, 1974 A manyfold increase in sister chromatid exchanges in bloom's syndrome lymphocytes. Proc. Natl. Acad. Sci. USA 71: 4508–4512.

Chen, J., D. N. Cooper, N. Chuzhanova, C. Ferec, and G. P. Patrinos, 2007 Gene conversion: mechanisms, evolution and human disease. Nat. Rev. Genet. 8: 762–775.

Delabaere, L., H. A. Ertl, D. J. Massey, C. M. Hofley, F. Sohail *et al.*, 2016 Aging impairs double-strand break repair by homologous recombination in Drosophila germ cells. Aging Cell 16: 320–328.

Delacote, F., and B. S. Lopez, 2008 Importance of the cell cycle phase for the choice of the appropriate DSB repair pathway, for genome stability maintenance: the trans-S double-strand break repair model. Cell Cycle 7: 33–38.

Do, A. T., and J. R. LaRocque, 2015 The role of *Drosophila* mismatch repair in suppressing recombination between diverged sequences. Sci. Rep. 5: 17601.

Do, A. T., J. T. Brooks, M. K. Le Neveu, and J. R. LaRocque, 2014 Double-strand break repair assays determine pathway choice and structure of gene conversion events in *Drosophila melanogaster*. G3 (Bethesda) 4: 425–432.

Drummond, J. T., G. M. Li, M. J. Longley, and P. Modrich, 1995 Isolation of an hMSH2-p160 heterodimer that restores DNA mismatch repair to tumor cells. Science 268: 1909–1912.

Ellis, N. A., M. Sander, C. C. Harris, and V. A. Bohr, 2008 Bloom's syndrome workshop focuses on the functional specificities of RecQ helicases. Mech. Ageing Dev. 129: 681–691.

Fishman-Lobell, J., and J. E. Haber, 1992 Removal of nonhomologous DNA ends in double-strand break recombination: the role of the yeast ultraviolet repair gene R*AD1*. Science 258: 480–484.

German, J., R. Archibald, and D. Bloom, 1965 Chromosomal breakage in a rare and probably genetically determined syndrome of man. Science 148: 506–507.

Gloor, G. B., C. R. Preston, D. M. Johnson-Schlitz, N. A. Nassif, R. W. Phillis *et al.*, 1993 Type I repressors of P element mobility. Genetics 135: 81–95.

Grabarz, A., J. Guirouilh-Barbat, A. Barascu, G. Pennarun, D. Genet *et al.*, 2013 A role for BLM in double-strand break repair pathway choice: prevention of CtIP/Mre11-mediated alternative nonhomologous end-joining. Cell Rep. 5: 21–28.

Gravel, S., J. R. Chapman, C. Magill, and S. P. Jackson, 2008 DNA helicases Sgs1 and BLM promote DNA double-strand break resection. Genes Dev. 22: 2767–2772.

Heyer, W. D., K. T. Ehmsen, and J. Liu, 2010 Regulation of homologous recombination in eukaryotes. Annu. Rev. Genet. 44: 113–139.

Holmes, A. M., and J. E. Haber, 1999 Double-strand break repair in yeast requires both leading and lagging strand DNA polymerases. Cell 96: 415–424.

Ivanov, E. L., and J. E. Haber, 1995 *RAD1* and *RAD10*, but not other excision repair genes, are required for double-strand break-induced recombination in *Saccharomyces cerevisiae*. Mol. Cell. Biol. 15: 2245–2251.

Janssen, A., G. A. Breuer, E. K. Brinkman, A. I. van der Meulen, S. V. Borden *et al.*, 2016 A single double-strand break system reveals repair dynamics and mechanisms in heterochromatin and euchromatin. Genes Dev. 30: 1645–1657.

Jinks-Robertson, S., M. Michelitch, and S. Ramcharan, 1993 Substrate length requirements for efficient mitotic recombination in *Saccharomyces cerevisiae*. Mol. Cell. Biol. 13: 3937–3950.

Johnson-Schlitz, D., and W. R. Engels, 2006 Template disruptions and failure of double holliday junction dissolution during double-strand break repair in *Drosophila* BLM mutants. Proc. Natl. Acad. Sci. USA 103: 16840–16845.

Johnson-Schlitz, D. M., C. Flores, and W. R. Engels, 2007 Multiple-pathway analysis of double-strand break repair mutations in *Drosophila*. PLoS Genet. 3: e50.

Jung, H., J. A. Lee, S. Choi, H. Lee, and B. Ahn, 2014 Characterization of the *Caenorhabditis elegans* HIM-6/BLM helicase: unwinding recombination intermediates. PLoS One 9: e102402.

Kappeler, M., E. Kranz, K. Woolcock, O. Georgiev, and W. Schaffner, 2008 *Drosophila* bloom helicase maintains genome integrity by inhibiting recombination between divergent DNA sequences. Nucleic Acids Res. 36: 6907–6917.

Karow, J. K., A. Constantinou, J. L. Li, S. C. West, and I. D. Hickson, 2000 The bloom's syndrome gene product promotes branch migration of holliday junctions. Proc. Natl. Acad. Sci. USA 97: 6504–6508.

Kass, E. M., and M. Jasin, 2010 Collaboration and competition between DNA double-strand break repair pathways. FEBS Lett. 584: 3703–3708.

Kitao, S., I. Ohsugi, K. Ichikawa, M. Goto, Y. Furuichi *et al.*, 1998 Cloning of two new human helicase genes of the RecQ family: biological significance of multiple species in higher eukaryotes. Genomics 54: 443–452.

Knoll, A., and H. Puchta, 2011 The role of DNA helicases and their interaction partners in genome stability and meiotic recombination in plants. J. Exp. Bot. 62: 1565–1579.

Krishna, S., B. M. Wagener, H. P. Liu, Y. C. Lo, R. Sterk *et al.*, 2007 Mre11 and Ku regulation of double-strand break repair by gene conversion and break-induced replication. DNA Repair (Amst.) 6: 797–808.

Kusano, K., M. E. Berres, and W. R. Engels, 1999 Evolution of the RECQ family of helicases. A *Drosophila* homolog, *DmBlm*, is similar to the human bloom syndrome gene. Genetics 151: 1027–1039.

Kusano, K., D. M. Johnson-Schlitz, and W. R. Engels, 2001 Sterility of *Drosophila* with mutations in the bloom syndrome gene complementation by Ku70. Science 291: 2600–2602.

Langland, G., J. Kordich, J. Creaney, K. H. Goss, K. Lillard-Wetherell *et al.*, 2001 The bloom's syndrome protein (BLM) interacts with MLH1 but is not required for DNA mismatch repair. J. Biol. Chem. 276: 30031–30035.

LaRocque, J. R., and M. Jasin, 2010 Mechanisms of recombination between diverged sequences in wild-type and BLM-deficient mouse and human cells. Mol. Cell. Biol. 30: 1887–1897.

Lo, Y. C., K. S. Paffett, O. Amit, J. A. Clikeman, R. Sterk *et al.*, 2006 Sgs1 regulates gene conversion tract lengths and crossovers independently of its helicase activity. Mol. Cell. Biol. 26: 4086–4094.

Luria, S. E., and M. Delbruck, 1943 Mutations of bacteria from virus sensitivity to virus resistance. Genetics 28: 491–511.

Lynch, M., and J. S. Conery, 2000 The evolutionary fate and consequences of duplicate genes. Science 290: 1151–1155.

Maloisel, L., F. Fabre, and S. Gangloff, 2008 DNA polymerase δ is preferentially recruited during homologous recombination to promote heteroduplex DNA extension. Mol. Cell. Biol. 28: 1373–1382.

Mazon, G., A. F. Lam, C. K. Ho, M. Kupiec, and L. S. Symington, 2012 The Rad1-Rad10 nuclease promotes chromosome translocations between dispersed repeats. Nat. Struct. Mol. Biol. 19: 964–971.

McIlwraith, M. J., E. Van Dyck, J. Y. Masson, A. Z. Stasiak, A. Stasiak *et al.*, 2000 Reconstitution of the strand invasion step of double-strand break repair using human Rad51 Rad52 and RPA proteins. J. Mol. Biol. 304: 151–164.

McVey, M., and S. E. Lee, 2008 MMEJ repair of double-strand breaks (director's cut): deleted sequences and alternative endings. Trends Genet. 24: 529–538.

McVey, M., J. R. LaRocque, M. D. Adams, and J. J. Sekelsky, 2004 Formation of deletions during double-strand break repair in *Drosophila* DmBlm mutants occurs after strand invasion. Proc. Natl. Acad. Sci. USA 101: 15694–15699.

McVey, M., S. L. Andersen, Y. Broze, and J. Sekelsky, 2007 Multiple functions of *Drosophila* BLM helicase in maintenance of genome stability. Genetics 176: 1979–1992.

Myung, K., A. Datta, C. Chen, and R. D. Kolodner, 2001 SGS1, the *Saccharomyces cerevisiae* homologue of BLM and WRN, suppresses genome instability and homeologous recombination. Nat. Genet. 27: 113–116.

Nassif, N., J. Penney, S. Pal, W. R. Engels, and G. B. Gloor, 1994 Efficient copying of nonhomologous sequences from ectopic sites via P-element-induced gap repair. Mol. Cell. Biol. 14: 1613–1625.

Nimonkar, A. V., A. Z. Ozsoy, J. Genschel, P. Modrich, and S. C. Kowalczykowski, 2008 Human exonuclease 1 and BLM helicase interact to resect DNA and initiate DNA repair. Proc. Natl. Acad. Sci. USA 105: 16906–16911.

Nimonkar, A. V., J. Genschel, E. Kinoshita, P. Polaczek, J. L. Campbell *et al.*, 2011 BLM-DNA2-RPA-MRN and EXO1-BLM-RPA-MRN constitute two DNA end resection machineries for human DNA break repair. Genes Dev. 25: 350–362.

Paques, F., and J. E. Haber, 1999 Multiple pathways of recombination induced by double-strand breaks in *Saccharomyces cerevisiae*. Microbiol. Mol. Biol. Rev. 63: 349–404.

Pedrazzi, G., C. Z. Bachrati, N. Selak, I. Studer, M. Petkovic *et al.*, 2003 The bloom's syndrome helicase interacts directly with the human DNA mismatch repair protein hMSH6. Biol. Chem. 384: 1155–1164.

Preston, C. R., C. C. Flores, and W. R. Engels, 2006 Differential usage of alternative pathways of double-strand break repair in *Drosophila*. Genetics 172: 1055–1068.

Rong, Y. S., and K. G. Golic, 2000 Gene targeting by homologous recombination in *Drosophila*. Science 288: 2013–2018.

Rong, Y. S., and K. G. Golic, 2003 The homologous chromosome is an effective template for the repair of mitotic DNA double-strand breaks in *Drosophila*. Genetics 165: 1831–1842.

Ryu, J. S., and H. S. Koo, 2016 Roles of *Caenorhabditis elegans* WRN helicase in DNA damage responses, and a comparison with its mammalian homolog: a mini-review. Gerontology 62: 296–303.

Ryu, T., B. Spatola, L. Delabaere, K. Bowlin, H. Hopp *et al.*, 2015 Heterochromatic breaks move to the nuclear periphery to continue recombinational repair. Nat. Cell Biol. 17: 1401–1411.

Shrivastav, M., L. P. De Haro, and J. A. Nickoloff, 2008 Regulation of DNA double-strand break repair pathway choice. Cell Res. 18: 134–147.

Spies, M., and R. Fishel, 2015 Mismatch repair during homologous and homeologous recombination. Cold Spring Harb. Perspect. Biol. 7: a022657.

Sugawara, N., E. L. Ivanov, J. Fishman-Lobell, B. L. Ray, X. Wu *et al.*, 1995 DNA structure-dependent requirements for yeast *RAD* genes in gene conversion. Nature 372: 84–86.

Sugawara, N., T. Goldfarb, B. Studamire, E. Alani, and J. E. Haber, 2004 Heteroduplex rejection during single-strand annealing requires Sgs1 helicase and mismatch repair proteins Msh2 and Msh6 but not Pms1. Proc. Natl. Acad. Sci. USA 101: 9315–9320.

Suzuki, T., M. Yasui, and M. Honma, 2016 Mutator phenotype and DNA double-strand break repair in BLM helicase-deficient human cells. Mol. Cell. Biol. 36: 2877–2889.

Symington, L. S., L. E. Kang, and S. Moreau, 2000 Alteration of gene conversion tract length and associated crossing over during plasmid gap repair in nuclease-deficient strains of *Saccharomyces cerevisiae*. Nucleic Acids Res. 28: 4649–4656.

Szostak, J. W., T. L. Orr-Weaver, R. J. Rothstein, and F. W. Stahl, 1983 The double-strand-break repair model for recombination. Cell 33: 25–35.

Wang, Y., S. Li, K. Smith, B. C. Waldman, and A. S. Waldman, 2016 Intrachromosomal recombination between highly diverged DNA sequences is enabled in human cells deficient in bloom helicase. DNA Repair (Amst.) 41: 73–84.

Ward, J. D., D. M. Muzzini, M. I. Petalcorin, E. Martinez-Perez, J. S. Martin *et al.*, 2010 Overlapping mechanisms promote postsynaptic RAD-51 filament disassembly during meiotic double-strand break repair. Mol. Cell 37: 259–272.

Wei, D. S., and Y. S. Rong, 2007 A genetic screen for DNA double-strand break repair mutations in drosophila. Genetics 177: 63–77.

Weinert, B. T., and D. C. Rio, 2007 DNA strand displacement, strand annealing and strand swapping by the *Drosophila* bloom's syndrome helicase. Nucleic Acids Res. 35: 1367–1376.

Wright, W. D., and W. D. Heyer, 2014 Rad54 functions as a heteroduplex DNA pump modulated by its DNA substrates and Rad51 during D loop formation. Mol. Cell 53: 420–432.

Wu, L., and I. D. Hickson, 2003 The bloom's syndrome helicase suppresses crossing over during homologous recombination. Nature 426: 870–874.

Wu, L., C. Z. Bachrati, J. Ou, C. Xu, J. Yin *et al.*, 2006 BLAP75/RMI1 promotes the BLM-dependent dissolution of homologous recombination intermediates. Proc. Natl. Acad. Sci. USA 103: 4068–4073.

Xie, J., S. L. Bessling, T. K. Cooper, H. C. Dietz, A. S. McCallion *et al.*, 2007 Manipulating mitotic recombination in the zebrafish embryo through RecQ helicases. Genetics 176: 1339–1342.

Yang, Q., R. Zhang, X. W. Wang, S. P. Linke, S. Sengupta *et al.*, 2004 The mismatch DNA repair heterodimer, hMSH2/6, regulates BLM helicase. Oncogene 23: 3749–3756.

Yin, Y., and T. D. Petes, 2014 The role of Exo1p exonuclease in DNA end resection to generate gene conversion tracts in *Saccharomyces cerevisiae*. Genetics 197: 1097–1109.

Communicating editor: J. Surtees